



Ionic Liquid Supported on DFNS Nanoparticles Catalyst in Synthesis of Cyclic Carbonates by Oxidative Carboxylation

Mengbing Cui¹ · Farzaneh Shamsa²

Received: 3 January 2021 / Accepted: 28 March 2021

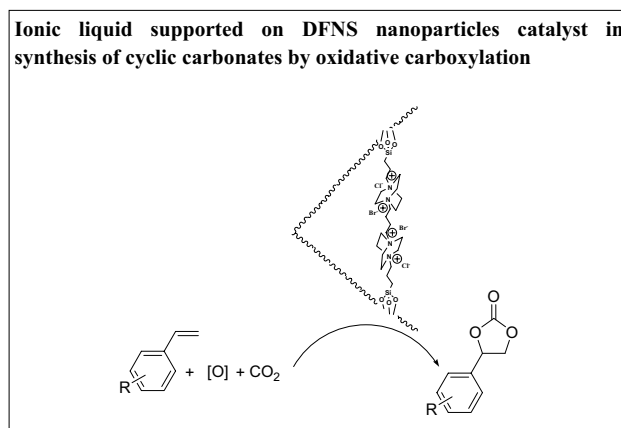
© The Author(s), under exclusive licence to Springer Science+Business Media, LLC, part of Springer Nature 2021

Abstract

In this paper, in the proximity of epoxides, we have suggested the conversion of carbon dioxide (CO₂) for cyclic carbonates known as the most proper approach for synthesizing this C1 building block. Oxidation carboxylation of styrenes with CO₂ is performed at aerobic conditions utilizing the present approach. Oxidize carboxylation of styrenes by CO₂ was performed in the presence of DFNS-IL as NPs. Good to superb performance products were provided deploying DFNS-IL nanocatalyst. In addition, the anatomy of DFNS-IL has been distinguished by various methods, including XRD, VSM, FT-IR, SEM, EDX, TEM, and TGA. The stability of the catalytic system increased after the excessive addition of DFNS. In addition, the hot filtration test provided complete insight into the heterogeneity of the catalyst. The reuse and recycling of the catalyst were repeatedly investigated for coupling reactions. In addition, the mechanism of the coupling reactions was thoroughly studied.

Graphic Abstract

Ionic liquid supported on DFNS nanoparticles catalyst in synthesis of cyclic carbonates by oxidative carboxylation



Keywords Nanocatalyst · Green chemistry · Carbon dioxide · Ionic liquids · DFNS

✉ Mengbing Cui
cuimengbing@163.com

✉ Farzaneh Shamsa
Farzaneh.Shamsa@gmail.com

¹ College of Pharmacy, Xinxiang University,
Xinxiang 453003, China

² New Materials Technology and Processing Research Center,
Department of Chemistry, Neyshabur Branch, Islamic Azad
University, Neyshabur, Iran

1 Introduction

The proper organic chemicals can be obtained by converting carbon dioxide known as a promising research area [1–5]. There organic chemicals are not a greenhouse gas emission or a waste material produced in chemical industries but also a non-flammable, non-toxic and readily available carbon raw material [6, 7]. However, in the conversion of CO₂ molecules, thermodynamically, they are not utilized in

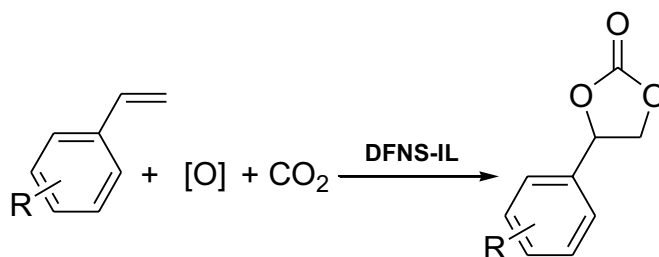
the industry due to the fact that CO_2 possesses low reactivity, high active catalysts, energy inputs, optimization conditions, etc. known as key factors [8].

In different industries, cyclic carbonates were widely used as electrolytes in intermediate organic synthesis, monomers, aprotic polar solvents and lithium batteries. In the recent years, many cyclic carbonate combinations were produced from CO_2 . Among them, the cycloaddition of CO_2 to epoxides was determined as a usual and industrial method [9, 10]. Because of the simply available and lower cost raw materials, alkenes as well as do not require the separation of epoxide, after the first step, direct production of cyclic carbonates from CO_2 and also olefins using oxidative carboxylation (refer to Scheme 1) consists a mixture of alkene epoxidation and CO_2 cycloaddition to epoxide production can be a more cost effective method [11–18]. Olefin oxidative carboxylation has been explored in 1962 but more studies on the cycloaddition of CO_2 to epoxide ring still require further studies [19–21].

As for morphology-controlled nanomaterials, dendritic fibrous nanosilica has been recently discovered by Polshettiwar et al. [22–24]. It depicted exceptional activities in all areas, including gas adsorption, catalysis, energy storage, solar-energy harvesting, biomedical applications and sensors. It is called dendrimeric silica fibers morphology (DFNS) considering the fibrous morphology reported in our previous report [25–28]. Since the fibers were thin sheets 3.5–5.2 nm thick, other names are deployed in the literature, including wrinkled, fibrous, dendritic, nanoflower, lamellar, and dandelion. In this study, to prevent confusion, we used the name employed in the respective original works. However, to maintain consistency, we use dendritic fibrous nanosilica as a common name for this family of materials. The uniform roots of DFNS roots in their dendritic fibrous morphology are more accessible in all dimensions and sides in comparison with the tubular pores of SBA-15 and MCM-41. This fibrous structure increases the active sites like metal oxides, metals, organic molecules, and organometallics in the outer layer of silica without blocking the channels. In addition, it allows more access to generated active sites. By modifying the particle size (40–1120 nm) and density of

fiber (number of fibers into one sphere), the DFNS outer layer area may alter from 450 to 1244 m^2g^{-1} [29]. It should be noted that unlike the erratic distribution of pores in usual silica materials, DFNS has oriented fibrous channels that increase in size from the center to the external layer. Controlling DFNS fiber density can adjust the volume and size of the pores. Its adjustable pore size in the range of 3.7–25 nm allows pores to fit the particular visitant molecules in different sizes, whilst its adjustable pore volume of 2.18 cm^3g^{-1} facilitates the high loadings of visitants [30, 31]. Visitants include organometallic complexes, organic molecules, metals, inorganic salts, peptides, metal oxides, enzymes, proteins, carbon, and polymers. The integrated porosity of DFNS accompany with its hierarchical pore arrangement including mesopores of various sizes (such as suitable amounts of macr- and micropores) helps the visitant molecules to efficiently adsorb and diffuse in the fibrous spheres with minimal constraints; it helps to increase the accessibility of active sites and the internal layer (a significant issue in usual mesoporous materials). Macropores contribute to the effective initial diffusion/adsorption of guest molecules and DFNS have proper stability (mechanical, chemical, hydrothermal, and thermal) toward usual mesoporous materials, which is a major concern due to their thin silica walls. DFNS is biocompatible as well as nontoxic. Particle size control facilitates partial modification of dispersion and realization of these nanospheres.

Dendrimers are popular in the domain of catalysis because of highly branched 3D anatomies, unique dendritic effects, and numerous peripheral categories [32, 33]. Immobilizing the dendrimer catalyst on support materials has attracted the attention of many chemists due to facile reusability and recoverability [34–36]. ILs have been extensively utilized in green chemistry due to their specific characteristics, including low vapor pressure, low burnability, firmness, etc. The ability to adjust anatomy and characteristics is the most significant property of ILs. The physical and chemical characteristics of ILs can be adjusted by introducing various functional groups into anions or cations with diverse anatomies. Dendritic ILs (DILs), which are a combination of the characteristics of dendrimers and ILs, have extensively



Scheme 1 Synthesis of cyclic carbonates through oxidative carboxylation of alkenes

utilized in the domain of catalysis, transporters, and adsorption of heavy metal cations [37, 38].

The current study reports the novel green approach for the synthesis of DFNS NPs immobilized by ILs based on 1,4-diazabicyclo[2.2.2]octane (DABCO), as DABCO is a medium-hindrance tertiary amine with cage-like anatomy. This anatomy was utilized as a cheap, green, highly reflexive, and non-poisonous catalyst for different ionic liquids. The findings illustrated the influence of IL on the nano anatomies and characteristics. This catalyst has many advantages, including facile separation, good activity, and selectivity for oxidation carboxylation of styrenes by using CO₂ under mild conditions (refer to Scheme 1).

2 Experimental

2.1 A Universal Approach for Providing DFNS Nanoparticles

Tetraethyl orthosilicate (TEOS) (3.5 g) was dissolved in a solution of cyclohexane (40 mL) and 1-pentanol (3.0 mL). Then, a mixed solution of cetylpyridinium bromide (CPB) (1.5 g) and urea (0.9 g) in H₂O (45 mL) was released and continually mixed for 45 min at room temperature. Next, it was located in a Teflon-sealed hydrothermal reactor and heated at 130 °C for 3 h. The generated silica was centrifuged then washed with a mixture of deionized water and acetone, and oven-dried. The material was then calcined in air at 600 °C for 6 h.

2.2 A Universal Approach for Providing DFNS/3-chloropropyltriethoxysilane Nanoparticles

A solution of 3 mmol of DFNS NPs and 30 mL tetrahydrofuran was made in a beaker, and then 30 mmol of NaH was released by ultrasonication. 30 mmol 3-chloropropyltriethoxysilane was dispersed drop-wise at r.t. and mixed for another 13 h at 75 °C. The final products were washed with ethanol and deionized water, respectively, and vacuum-dried at 60 °C for 2 h.

2.3 Synthesis of 4,40-(butane-1,4-diyl) bis-1,4-diazabicyclo[2.2.2]octane-1,4-diium(IL)

A blend of ethylacetate (15 ml), 1,4-dibromobutane (3.0 mmol) and 1,4-diazabicyclo[2.2.2]octane (DABCO) (7 mmol) were mixed at r.t. for 20 h. The white precipitate was isolated, suspended in 15 ml of anhydrous tetrahydrofuran, and stirred at 30 °C. After 2 h, the solvent was eliminated by centrifugation and the solid was dried at room temperature (melting point of ionic liquid = 247–249 °C).

2.4 Synthesis of DFNS-IL Catalyst

First, DFNS was sonicated in toluene (15 ml) for 40 min. The provided ionic liquid (3.0 mmol) was then released and the reaction was continued for 68 h under reflux situations. Upon completion, the resulting precipitate was isolated employing an external magnet and washed with 15 ml of ethanol to eliminate the unreacted ionic liquid. The resulting solids were dried at r.t. and employed as the catalyst in providing quinazolinone derivatives.

2.5 Catalytic Reactions

The related reaction was done into a stainless autoclave (by the volume of 25 mL). Twenty millimole olefin, and 10 mg DFNS-IL were used in the stainless autoclave. The obtained compound was then stirred utilizing a magnetic stirrer. After that, it was laced in a water bath and was heated to the appropriate temperature. For many times, reactor was purged by CO₂ and charged by CO₂. After that, the stainless autoclave was heated to an appropriate temperature and stirred for a half of hour. After the reaction was finished, the reactor is then cooled to the temperature of 25 °C, and the remained CO₂ was slowly discharged from the reactor. The obtained solution from the reaction was evaluated using GC–MS and GC.

3 Results and Discussion

The synthesis of DFNS-IL NPs was a multi-step process. The fibers of DFNS has several Si–OH groups on the outer layers. Therefore, the DFNS rapidly functionalized with 3-chloropropyltriethoxysilane and produced DFNS/3-chloropropylsilane NPs. Then, with DABCO support on DFNS/3-chloropropylsilane nanoparticles, DFNS-IL catalyst was synthesized in a simple and cheap procedure that is characterized by easy access to active sites and high catalytic activity (Scheme 2).

The anatomies of the synthesized DFNS, and DFNS-IL NPs were investigated by SEM and TEM. The DFNS microspheres with fibrous anatomy were identical and monodispersed (Fig. 1a). The average diameter of the microspheres was about 200–250 nm. TEM and SEM pictures (Fig. 1a and c) further illustrate that the two fibers were approximately 10–20 nm apart. The SEM pictures of DFNS-IL NPs show that rectification did not change the morphology of DFNS (Fig. 1b and d); however, discrete nanospheres grew as twins.

FT-IR spectroscopy was deployed to discover the changes in the level of the synthesized catalyst (Fig. 2). The bands at 799, 1086, and 1662 cm⁻¹ in the FT-IR spectrum of both DFNS and DFNS-IL corresponds to the

tensile state of typical silanol group (Si–OH), Si–O–Si vibrations, and the water absorbed on the solid outer layer, respectively (Fig. 2a and b). Robust absorption bands at 1615 and 1458 cm^{-1} were differentiated from C–N and C–C vibrations of the DABCO section. The absorption bands were related to the different (C–H) bonds like N–CH₂, CH₂–CH₂ and C–H emerged at 2896, 2972, 3062 cm^{-1} . These observations affirmed that the silica-coated outer layer of the DFNS was strongly altered with the 4,40-(butane-1,4-diyl)bis-1,4-diazabicyclo[2.2.2]octane-1,4-dium) as ionic liquids.

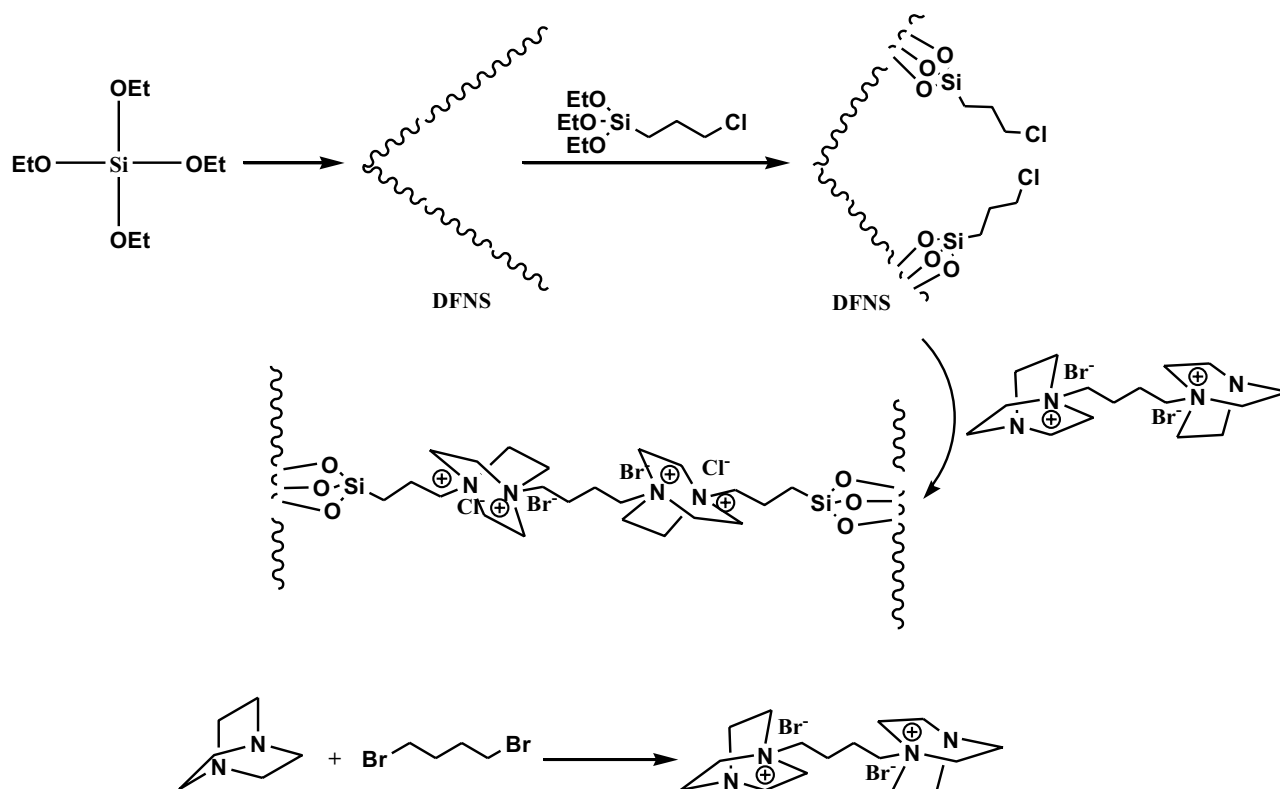
Figure 3 shows the TG analysis of DFNS-IL NPs. The TG curve of DFNS-IL NPs illustrated weight reduction at 70 °C to 280 °C, which corresponded to the water molecules adsorbed in the support. The organic group functionalized analogs DFNS-IL experienced notable weight loss (32%) at ~400 °C, possibly because of ligand decomposition.

We utilized XPS to examine the chemical sections on the DFNS-IL NPs level. Figure 4 shows a scheme of XPS for the gathered catalyst. Peaks Cl, C, O, N, and Br can be seen and the attendance of N 1s additional affirms that DFNS were functionalized employing DABCO. In addition, the presence of ions of Br[−] (the DABCO counter ion) was determined by an edged apex. This shows the presence of DABCO in the catalyst. Figure 5 illustrates the origins of the catalyst that

was specified by EDX analysis. Figure 5 illustrates the elements in DFNS-IL NPs such as nitrogen, silicon, oxygen, carbon, chlorine, and bromine. The NPs outer layer roughness was determined by atomic force microscopy (AFM) analysis. Figure 6 illustrates the topographic scheme. The higher altitude region, shown in bright yellowish white, was increased by reducing T/W. This indicated an enhancement in the unevenness of the catalyst's outer layer.

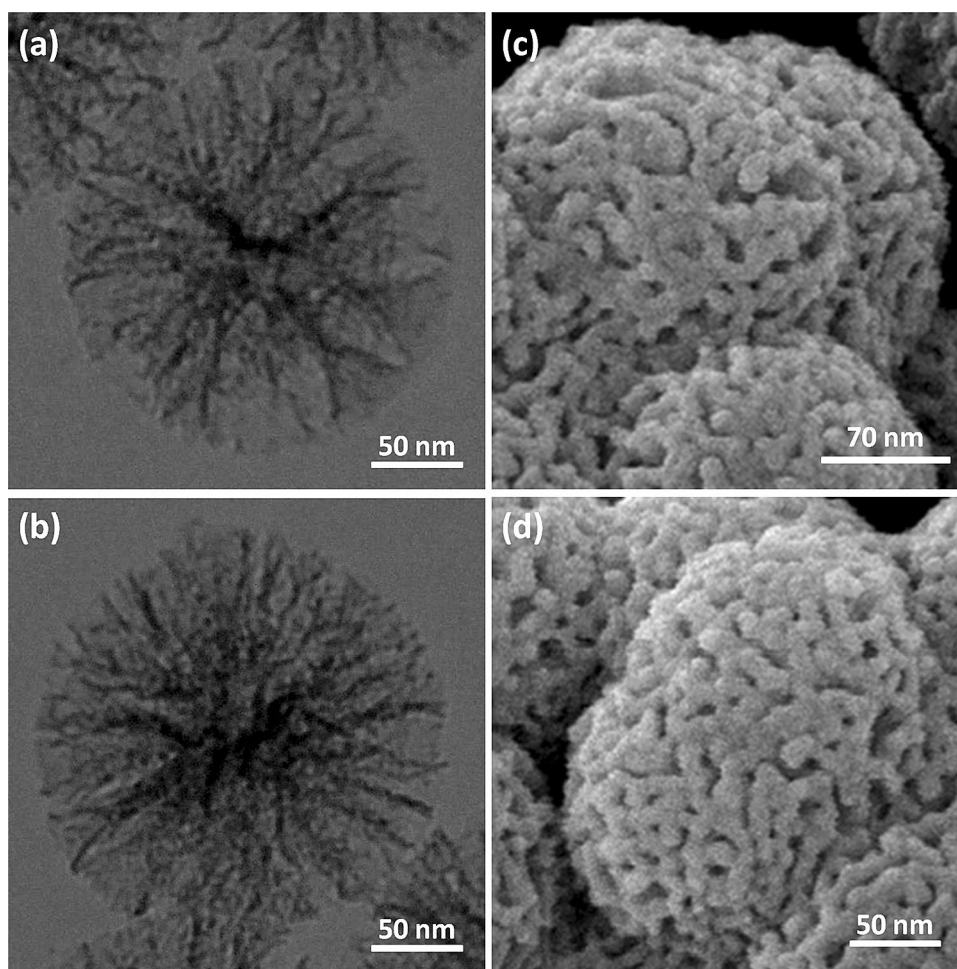
Nitrogen adsorption–desorption isotherm analysis was performed to investigate the particular outer layer area and porosity of the products. Following the BJH approach, the mean pore diameter, the particular outer layer area, and the total pore volume values were determined (Table 1). The BET findings illustrated that the active outer layers of the DFNS and DFNS-IL are 632 and 309 $\text{m}^2 \text{g}^{-1}$, respectively. The results demonstrated that the specific outer layer reduced after DABCO intercalation. Moreover, the pore volume and average pore radius reduced by employing DABCO. DABCO intercalation was found to have more porous network anatomy.

Impressive elements like the catalyst amount, oxidant and solvent for the oxidation carboxylation of styrenes with CO₂ known as a model reaction are investigated for obtaining the optimum conditions in terms of the oxidation reactions. Many solvents are utilized for studying the related effect



Scheme 2 Preparation of DFNS-IL nanocatalyst

Fig. 1 TEM pictures of **a** DFNS and **b** DFNS-IL NPs; SEM pictures of **c** DFNS and **d** DFNS-IL NPs



onto the production of cyclic carbonates and no considerable product is synthesized by polar protic solvents like 2-propanol, methanol, ethanol and water. Polar protic solvents like EtOAc, DMSO, and DMF demonstrated mild efficiency in cross-coupling products. It is found that solvents are less efficient compared to usual heating under solvent-free states. The cross-coupling reaction performance of carbonylation is higher in less polar solvents like toluene or anisole. A constant amount of catalyst (10.0 mg) is enough to obtain the quantitative performance of product. Lower amounts obtained in lower yields. The significance and the influence of the catalyst is proved while the reaction at the existence of the catalyst demonstrated no efficiency. Noted that, cases of all reactions, a selectivity of more than average 99% to product is archived. The selective production of cyclic carbonate demonstrated the highest efficiency for around 25 min at 25 °C under an open air atmosphere. In Table 2, there are not oxidants of additives in the case of this conversion.

The pressure of CO₂ possessed a considerable impact on the parallel reaction. Table 3 shows that the rate of reaction rapidly enhanced considering the pressures among 0.5

and 1.0 MPa. Based on previous studies, it is found that the enhancement of reaction pressure until the pressure is under 1.0 MPa is determined very favorable in the case of cyclic carbonate production. Hence, 1.0 MPa CO₂ pressure is specified as a special condition. For increasing yields of product, many oxidants are utilized. The yield of reaction is dramatically sensitive to the oxidant. Noted that, the basicity of catalyst is not known as a parameter for specifying activity. As can be seen in Table 3, the highest yield is determined by utilizing oxygen as an oxidant. In addition, the production of cyclic carbonate enhanced around 99% under the temperature of 60 °C and 1.0 MPa CO₂ pressure at 25 min. It should be noted that more enhancement in temperature caused in a low reduction in the yields of the product because of an insignificant value of specific byproducts like olefin isomerization. Hence, in the case of the parallel reactions of olefin and CO₂, the optimum temperature is determined to be 60 °C.

As can be seen in Table 4, in this novel one-pot approach, many olefins are studied in cases of the substrate scopes to produce cyclic carbonates. Noted that, for all considered

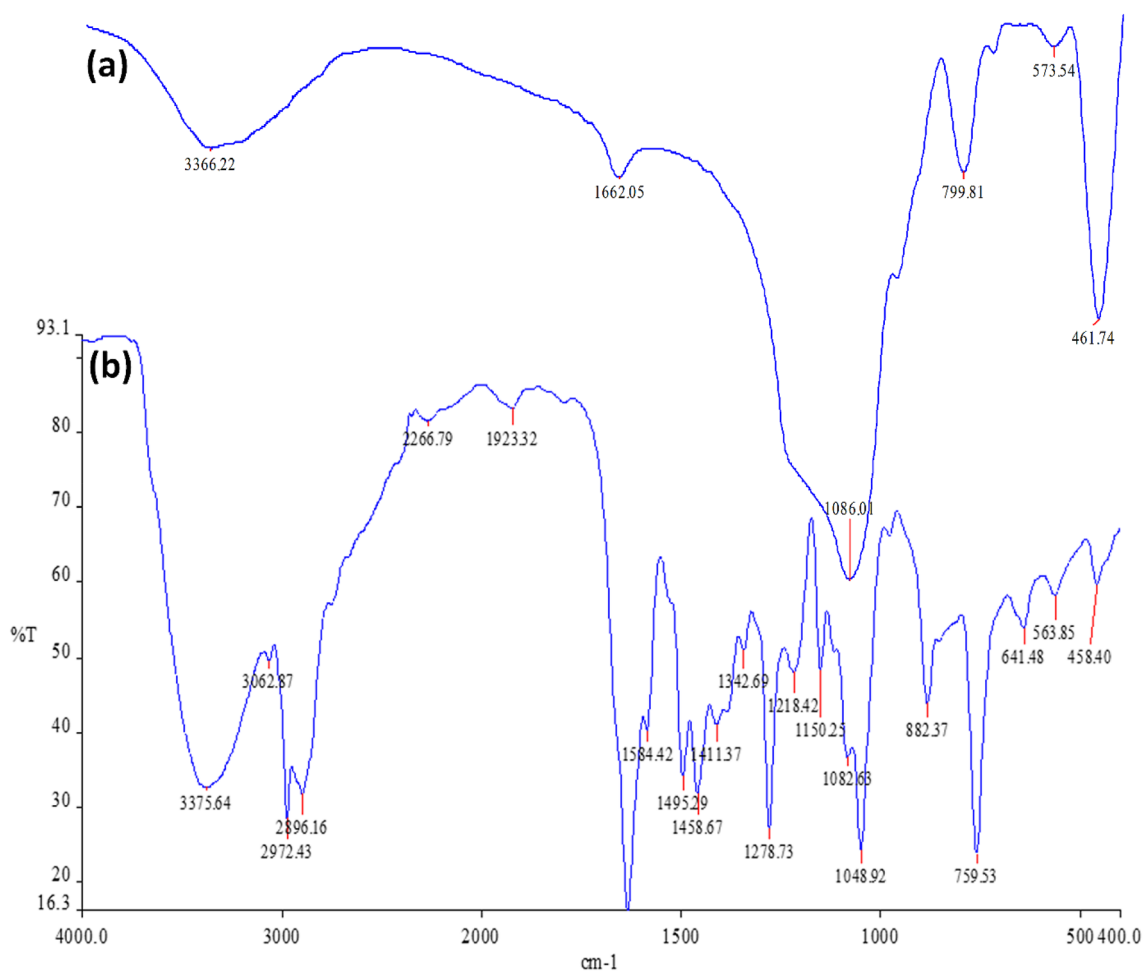


Fig. 2 FTIR spectra of **a** DFNS; **b** DFNS-IL NPs

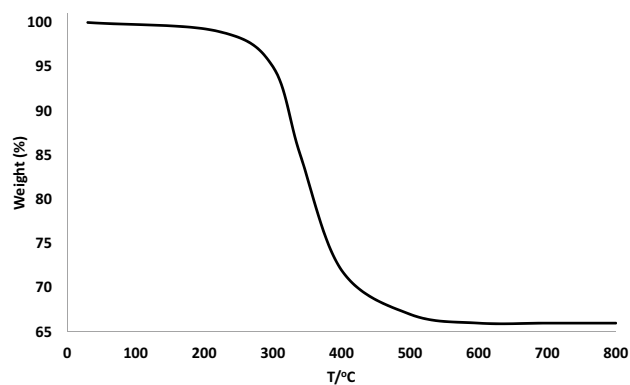


Fig. 3 TGA diagram of DFNS-IL NPs

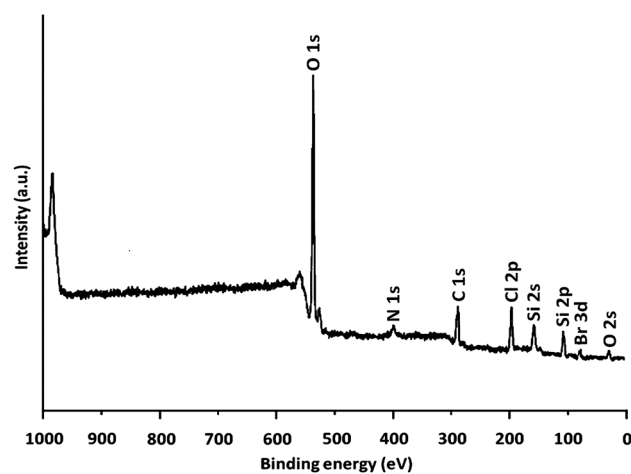


Fig. 4 XPS spectra of DFNS-IL NPs

substrates, the catalyst is active. In addition, aryl olefins bearing a para-chloro group have been introduced as proper substrates provided near-quantitative products. Aryl olefins and also the meta or ortho-chloro groups, are additionally

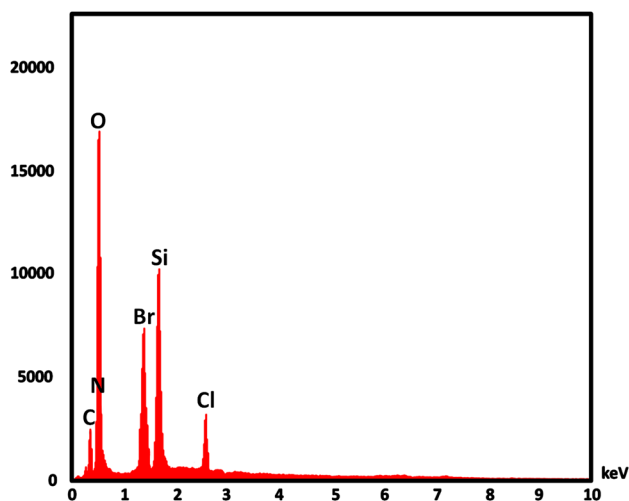


Fig. 5 EDX spectra of DFNS-IL NPs

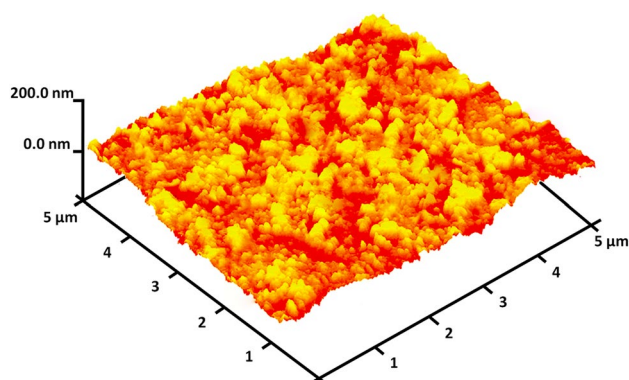


Fig. 6 3D AFM cultivars of DFNS-IL NPs

Table 1 Anatomical parameters of DFNS, and the DFNS-IL NPs

Catalysts	S_{BET} ($\text{m}^2 \text{g}^{-1}$)	V_a ($\text{cm}^3 \text{g}^{-1}$)	D_{BJH} (nm)
DFNS	632	3.0	13
DFNS-IL	309	1.2	7

appropriate substrates. Whereas an electron-donating group like methyl over the aryl group reduced the product yield.

For a deeper evaluation of the efficiency of the catalyst, various control experiments were conducted and the results are shown in Table 5. The reaction performed deploying DFNS showed that no amount of the product was formed after 25 min (Table 5, row 1). Moreover, no reaction was perceived when DFNS/3-chloropropyl as catalyst was employed (Table 5, row 2). 3-chloropropyl is not able to show good catalytic activity under standard reactions. Due to these unfavorable results, we continued research to increase efficiency by adding IL (Table 5, row 3). Our results show

Table 2 The effect of solvent, amount of catalyst, time, and temperature for synthesis of cyclic carbonate

Entry	Solvent	Catalyst (mg)	Time (min)	Yield (%) ^a
1	EtOH	20	45	–
2	MeOH	20	45	–
3	i-PrOH	20	45	–
4	H ₂ O	20	45	–
5	DMF	20	60	31
6	THF	20	60	42
7	DMSO	20	60	79
8	Dioxane	20	70	–
9	CH ₃ CN	20	60	47
10	CH ₂ Cl ₂	20	70	54
11	EtOAc	20	70	58
12	Toluene	20	60	18
13	CHCl ₃	20	50	79
14	n-Hexane	20	50	–
15	Benzene	20	70	13
16	CCl ₄	20	70	20
17	Cyclohexane	20	70	22
18	Solvent-free	20	45	99
19	Solvent-free	15	45	99
20	Solvent-free	10	45	99
21	Solvent-free	5	45	92
22	Solvent-free	10	35	99
23	Solvent-free	10	25	99
24	Solvent-free	10	15	73

^aGC yields [%]

Table 3 Effect of oxidant, CO₂ pressure, and temperature on the carboxylation of styrenes with CO₂

Entry	Oxidant	CO ₂ Pressure (MPa)	Temperature (°C)	Yield (%) ^a
1	O ₂	2.0	80	99
2	TBHP	2.0	80	91
3	H ₂ O ₂	2.0	80	42
4	Oxone	2.0	80	–
5	KIO ₄	2.0	80	–
6	NaOCl	2.0	80	27
7	Air	2.0	80	–
8	O ₂	1.5	80	99
9	O ₂	1.0	80	99
10	O ₂	0.5	80	35
11	O ₂	1.0	70	99
12	O ₂	1.0	60	99
13	O ₂	1.0	50	90

^aGC yields [%]

that the reaction cycle is primarily catalyzed using IL in the DFNS nanostructure. Nanoparticles increase the activity of the catalyst due to the increase in surface area to volume, so they significantly increase the sensitivity between the

reactants and the catalyst and act as a homogeneous catalyst (Table 5, rows 3 and 4).

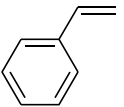
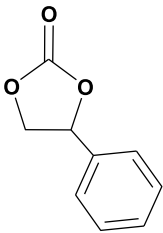
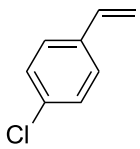
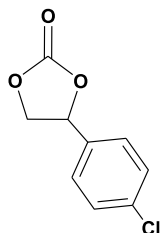
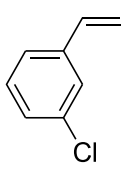
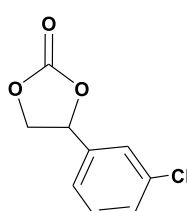
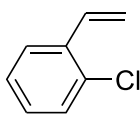
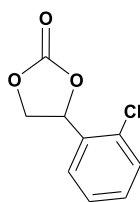
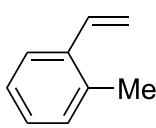
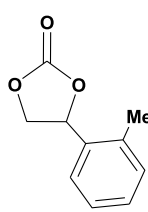
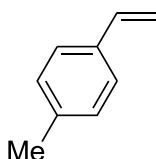
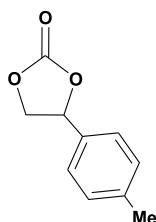
The catalytic activity of DFNS-IL NPs was compared with other reported catalysts used for carboxylation of styrenes with CO₂ (Table 6). Our outcomes proved that DFNS-IL had the best performance of product in different solvent, temperature, and time, which confirmed that our catalyst was more active.

In green chemistry, the catalyst recyclability is known an effective characteristic. Hence, the MNPs of DFNS-IL recyclability is evaluated to synthesis the cyclic carbonate. After the completion of the reaction, the solid MNPs of DFNS-IL are removed simply from the liquid reaction area at only few seconds, which can be recycled immediately after cleaning the solvent. In Figs. 7, 10 runs in a row reuse of the catalyst is shown. The efficiency of the product in the 10 th run is determined equal to 98% that demonstrated merely a 6% reduction with the efficiency of 92%.

We also performed a complete study on the catalyst heterogeneous nature. At first step, the hot filtration experiment for production of cyclic carbonate is performed under premium states and indicated that the catalyst is removed, magnetically, in situ after near 73% (for around 15 min removal). In order to tolerate more reaction, the reactants were permissible. It is determined that the free catalyst remnant determined to be fairly active, and 75% conversion is detected after 25 min of the cyclic carbonate production after removing the heterogeneous catalyst. We found that, in the process of reaction, the catalyst heterogeneously worked and unwilling just low leaching done in the reaction (Fig. 8).

The SEM and TEM image analysis illustrated the higher numbers of the fibrous nanoparticles of DFNS-IL. Figure 9a and b depict the SEM and TEM pictures of the new fibrous nanoparticles of DFNS-IL, and the ten-times recycled DFNS-IL. The fibrous anatomy of the catalyst was still visible after ten reuses and did not differ from fresh nanoparticles after ten consecutive uses. This can be attributed to strong recyclability. Moreover, the thermal stability of the recycled DFNS-IL catalyst was not as good as the fresh

Table 4 Cycloaddition of CO₂ with terminal olefins^a

Entry	Olefins	Products	Yield (%)
1			99
2			94
3			96
4			92
5			97
6			99

^aReaction conditions: appropriate CO₂ (1.0 MPa), aniline (1.0 mmol), DFNS-IL (10 mg), and under 60 °C.

Table 5 Influence of different catalysts for carboxylation of styrenes with CO₂^a

Entry	Catalyst	Yield (%) ^b
1	DFNS	-
2	DFNS/3-chloropropyl	-
3	DFNS-IL	99
4	IL	97

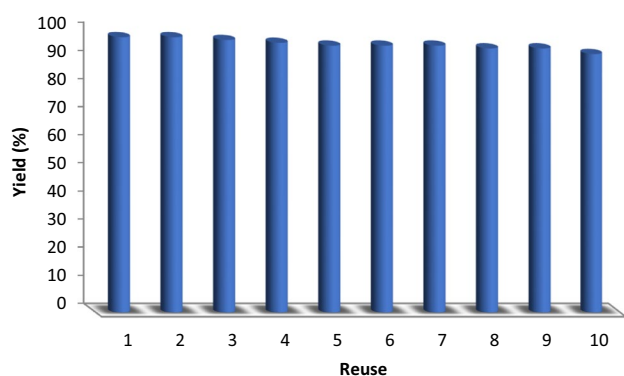
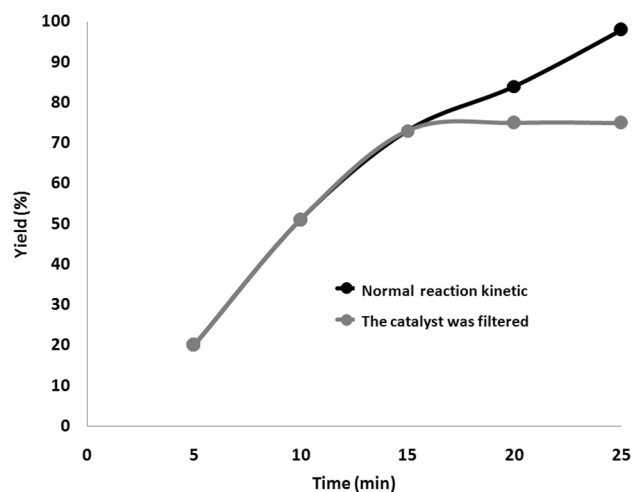
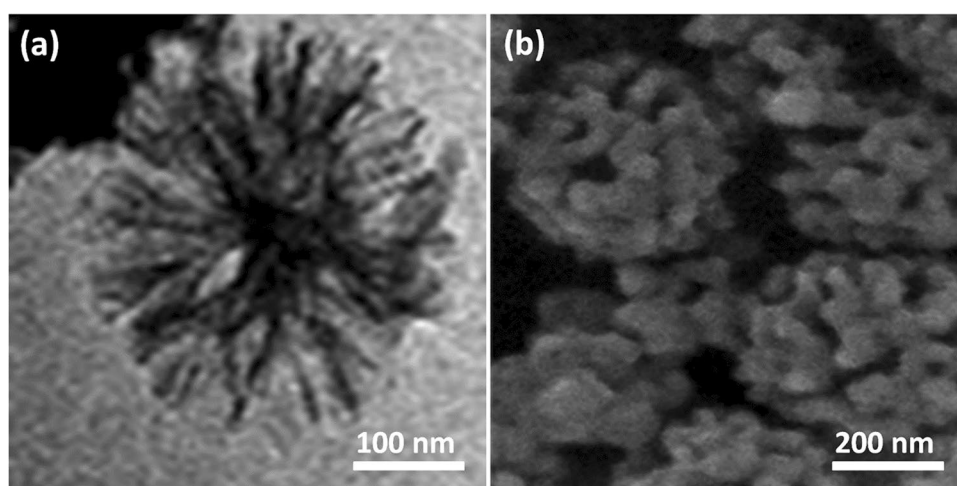
^aReaction conditions: CO₂ (1.0 MPa), aniline (1.0 mmol), and catalysts (10 mg), under 60 °C

^bIsolated yield

Table 6 Comparing the catalytic efficiency of DFNS-IL NPs to many catalysts^a

Entry	Catalyst	Temp	Time (h)	Solvent	Yield (%)
1	Fe(III)@MOF1	50	24–48	DCM	69 [39]
2	[C _n C _m Im][HCO ₃]	65	30	TBHP	63 [40]
3	[ZnW ₁₂ O ₄₀] ⁶⁻	50	96	–	82 [41]
4	Co(acac) ₂ -QPB@MCS	100	10	MeCN	77 [42]
5	Ti-MMM-E	70	48	–	49 [43]
6	[Ru(TPP)(O) ₂]	30	48	DCM	53 [14]
7	manganese(III)-complex	100	6	MeCN	32 [44]
8	NBS/DBU	60	3–6	H ₂ O	70 [45]
9	DFNS-IL	60	1	–	99

^aReaction conditions: cycloaddition of CO₂ in different solvent, temperature, and time

**Fig. 7** The reusability of catalysts for synthesis of cyclic carbonate**Fig. 8** Reaction kinetics, and hot filtration studies for synthesis of cyclic carbonate**Fig. 9** **a** TEM and **b** FE-SEM pictures of the improved DFNS-IL NPs after the tenth run for synthesis of cyclic carbonate

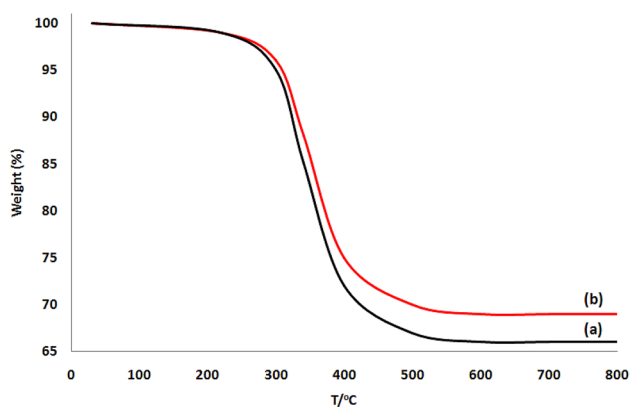


Fig. 10 TGA of the fresh DFNS-IL catalyst (a) and the recycled DFNS-IL catalyst after 10 times reusing (b)

catalyst after ten uses. This may be due to the loss of IL in DFNS fibers during recycling (Fig. 10). Fortunately, its performance does not change at 100 °C.

4 Conclusions

In summary, a novel class of DFNS was reported with support for ionic liquids based on ligands of DABCO groups, which exhibits tremendous catalytic activity for provide cyclic carbonate in excellent efficiency. SEM, TEM, FTIR, XPS, ICP-MS, BET, TGA, and EDX indicated the functionalization of IL in the outer layer of the mesopores silica. Moreover, the catalyst was reusable and easily recoverable. Such a logical design for single-site catalysts with full employment of any IL active site, superb reusability, and insignificant catalyst leaching are consistent with the concepts of green chemistry. Therefore, the study of DFNS-IL may create a potential basis for the fabrication of other readily available nanocatalyst that would be robustly efficient in different nanocatalyst-based reactions. This process might lead to the production of nanocatalysts with desirable characteristics, including efficiency and ease of reuse.

Acknowledgements The study was supported by “National Natural Science Foundation of China”, No.21706226

References

1. Zevenhoven R, Eloneva S, Teir S (2006) *Catal Today* 115:73–79
2. Sadeghzadeh SM, Zhiani R, Emrani S (2018) *Catal Lett* 148:119–124
3. Saadati SM, Sadeghzadeh SM (2018) *Catal Lett* 148:1692–1702
4. He LN, Wang JQ, Wang JL (2009) *Pure Appl Chem* 81:2069–2080
5. Sakakura T, Kohno K (2009) *Chem Commun* 11:1312–1330
6. Halmann MM, Steinberg M (1999) *Greenhouse gas carbon dioxide mitigation: science and technology*. Lewis Publishers, Boca Raton
7. Bakker D, Watson A (2001) *Nature* 410:765–766
8. Song C (2006) *Catal Today* 115:2–32
9. Lu XB, Darensbourg DJ (2012) *Chem Soc Rev* 41:1462–1484
10. Song QW, Zhou ZH, He LN (2017) *Green Chem* 19:3707–3728
11. Xiang D, Liu X, Sun J, Xiao F-S, Sun J (2009) *Catal Today* 148:383–388
12. Aresta M, Quaranta E (1987) *J Mol Catal* 41:355–359
13. Aresta M, Dibenedetto A, Tommasi I (2000) *Appl Organomet Chem* 14:799–802
14. Bai D, Jing H (2010) *Green Chem* 12:39–41
15. Sun JM, Fujita S, Bhanage BM, Arai M (2004) *Catal Today* 93:383–388
16. Sun JM, Fujita S, Bhanage BM, Arai M (2004) *Catal Commun* 5:83–87
17. Zalomaeva OV, Maksimchuk NV, Chibiryaev AM, Kovalenko KA, Fedin VP, Balzhinimaev BS (2013) *J Energy Chem* 22:130–135
18. Fukuoka S, Kawamura M, Komiya K, Tojo M, Hachiya H, Hasegawa K, Aminaka M, Okamoto H, Fukawa I, Konno S (2003) *Green Chem* 5:497–507
19. Coates GW, Moore DR (2004) *Angew Chem Int Ed* 43:6618–6639
20. Dai WL, Luo SL, Yin SF, Au CT (2009) *Appl Catal A* 366:2–12
21. North M, Pasquale R, Young C (2010) *Green Chem* 12:1514–1539
22. Polshettiwar V, Cha D, Zhang X, Basset JM (2010) *Angew Chem* 49:9652–9656
23. Maity A, Polshettiwar V (2017) *Chemsuschem* 10:3866–3913
24. Kundu PK, Dhiman M, Modak A, Chowdhury A, Polshettiwar V (2016) *ChemPlusChem* 81:1142–1146
25. Gautam P, Dhiman M, Polshettiwar V, Bhanage BM (2016) *Green Chem* 18:5890–5899
26. Fihri A, Cha D, Bouhrara M, Almana N, Polshettiwar V (2012) *Chemsuschem* 5:85–89
27. Zhiani R, Saadati SM, Zahedifar M, Sadeghzadeh SM (2018) *Catal Lett* 148:2487–2500
28. Sadeghzadeh SM (2016) *J Mol Liq* 223:267–273
29. Sadeghzadeh SM, Zhiani R, Moradi M (2018) *ChemistrySelect* 3:3516–3522
30. Baghbamidi SE, Hassankhani A, Sanchooli E, Sadeghzadeh SM (2018) *Appl Organomet Chem* 32:e4251
31. Dong Z, Le X, Li X, Zhang W, Dong C, Ma J (2014) *Appl Catal B* 158–159:129–135
32. Astruc D, Boisselier E, Ornelas C (2010) *Chem Rev* 110:1857–1959
33. Tomalia DA (2012) *New J Chem* 36:264–281
34. Giacalone F, Campisciano V, Calabrese C, Parola VL, Syrgiannis Z, Prato M (2016) *ACS Nano* 10:4627–4636
35. Sadjadi S, Malmir M, Heravi MM (2019) *Appl Clay Sci* 168:184–195
36. Murugan E, Jebaranjitham JN, Raman KJ, Mandal A, Geethalakshmi D, Kumarc MD, Saravanakumarc A (2017) *New J Chem* 41:10860–10871
37. Qin TY, Li XY, Chen JP, Zeng Y, Yu TJ, Yang GQ, Li Y (2014) *Chem Asian J* 9:3641–3649
38. Hayouni S, Robert A, Maes C, Conreux A, Marin B, Mohamadou A (2018) *New J Chem* 42:18010–18020
39. Sharma N, Dhankhar SS, Kumar S, Kumar TD, Nagaraja CM (2018) *Chem Eur J* 24:16662–16669
40. Liu J, Yang G, Liu Y, Wu D, Hu X, Zhang Z (2019) *Green Chem* 21:3834–3838

41. Han Q, Qi B, Ren W, He C, Niu J, Duan C (2015) *Nat Commun* 6:10007
42. Kumar S, Singhal N, Singh RK, Gupta P, Singh R, Jain SL (2015) *Dalton Trans* 44:11860–11866
43. Maksimchuk NV, Ivanchikova ID, Ayupov AB, Kholdeeva OA (2016) *Appl Catal B* 181:363–370
44. Ramidi P, Felton CM, Subedi BP, Zhou H, Tian ZR, Gartia Y, Pierce BS, Ghosh A (2015) *J CO2 Util* 9:48–57
45. Eghbali N, Li CJ (2007) *Green Chem* 9:213–215

Publisher's Note Springer Nature remains neutral with regard to jurisdictional claims in published maps and institutional affiliations.